Transport properties of a biphenyl-based molecular junction system—the electrode metal dependence

2009 J. Phys.: Condens. Matter 21 064220

(http://iopscience.iop.org/0953-8984/21/6/064220)

J. Phys.: Condens. Matter **21** (2009) 064220 (5pp) doi:10.1088/0953-8984/21/6/064220

Transport properties of a biphenyl-based molecular junction system—the electrode metal dependence

Hisashi Kondo[1,2], **Jun Nara**[1], **Hiori Kino**[1] **and Takahisa Ohno**[1,2,3]

[1] CMSC, National Institute for Materials Science (NIMS), Tsukuba, Ibaraki 305-0047, Japan
[2] Institute of Industrial Science, University of Tokyo, Meguro, Tokyo 153-8505, Japan
[3] MANA, National Institute for Materials Science (NIMS), Tsukuba, Ibaraki 305-0047, Japan

Received 29 June 2008, in final form 2 December 2008
Published 20 January 2009
Online at stacks.iop.org/JPhysCM/21/064220

Abstract

We investigate the transport properties of a biphenyl-dithiol molecule sandwiched between electrodes made of metal Y (Y = Cu, Ag and Au) using the non-equilibrium Green's function method based on a density functional theory. The electrode metal Y has an influence on the coupling between the molecule and electrodes, and thus on the transmission peak height. For the transmission T_Y at the Fermi energy, we obtain $T_{Cu} \sim T_{Ag} < T_{Au}$. As a result, the current value at low bias voltage for the junction system with Ag or Cu electrodes is smaller than that for Y = Au. At high bias voltage, on the other hand, the current value of an Ag electrode system becomes larger than the others due to the higher transmission peak around −1.5 eV below the Fermi energy. Besides this, it is shown that the transmission peak value for all the electrode metals can be expressed generally as a function of a ratio of the coupling between the two phenyl rings to the peak width of the projected density of states with respect to a corresponding molecular orbital.

(Some figures in this article are in colour only in the electronic version)

1. Introduction

Transport properties have been investigated theoretically and experimentally for a wide variety of junction systems composed of a molecule and metal electrodes [1–3]. Their functionalities, which are related to molecular devices [4] and spintronics [5], have also been theoretically discussed. It is well known that such transport properties are very sensitive to the constituent materials. Therefore, it is useful for future research to organize the dependence of the transport properties on constituent materials.

Already, the electrode metal dependence of the transport properties for a benzene-based molecule has been theoretically investigated [6–9]. In [6], the transport properties of an α,α'-xylyl-dithiol molecule sandwiched between Au electrodes were compared with those of a system with Ag electrodes. For a system with Au electrodes, a larger transmission at the Fermi energy has been obtained. Besides this, it was reported that a system with Ag electrodes has a weaker interaction between the molecule and the electrode.

Recently, the transport properties of a biphenyl-dithiol (BPD) molecule sandwiched between Au electrodes, as shown in figure 1(a), were theoretically investigated [10–13]. The transport properties of this system strongly depend on the dihedral angle between the two phenyl rings of a BPD molecule, since the coupling between molecular orbitals (MOs) on the phenyl rings strongly depends on them. In [14], the end-group atom dependence of the transport properties for a biphenyl-based molecular system was investigated. As the end-group atom, O, S, Se and Te were studied. It has been shown that an end-group atom has an influence on not only the coupling between MOs on the phenyl rings but also the interaction between molecule and electrode. In the system with the O atom, which has a weaker molecule–electrode interaction and a stronger coupling between the MOs on the phenyl rings, a larger transmission at the Fermi energy has been obtained. In [15], it has also been reported that the transmission peak value strongly depends on the distance between the molecule and the electrode, and thus on the molecule–electrode interaction[4]. In this way, the transport properties of a

[4] The electron scattering inside a biphenyl-based molecule strongly depends on the interaction between the phenyl rings, as shown in [10–14]. This scattering becomes more pronounced with increase in the molecule–electrode interaction. The mechanism of this phenomenon is reported in [15].

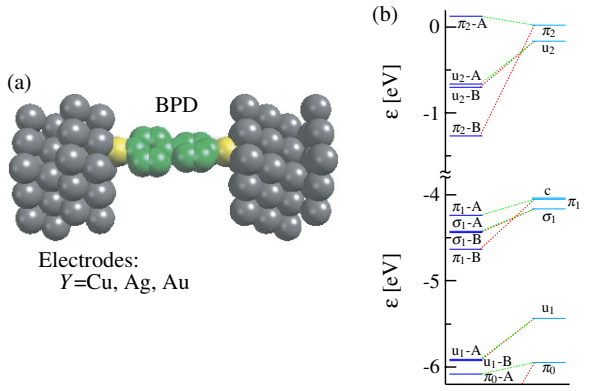

Figure 1. (a) Atomic structure for a BPD molecular junction system. (b) MO levels of an isolated BPD molecule (left), accompanied by MO levels of a half-fragment of a BPD molecule (right). Details of the labels, such as σ_1 and π_1, are given in the text.

biphenyl-based molecular junction system strongly depend on the molecule–electrode interaction. In these previous reports, however, only Au was used as the electrode metal that has an influence on a molecule–electrode interaction. It is of interest how the transport properties depend on the electrode metal.

In the present study, we theoretically investigate the electrode metal Y dependence of the transport properties of a BPD molecular system and then the relation between the transport properties and the molecule–electrode interaction is discussed. As the electrode metal Y, Cu, Ag and Au are studied.

2. Calculation method

In order to study the transport properties, we employ the non-equilibrium Green's function method based on a density functional theory (NEGF/DFT) [14][5]. We briefly describe this method in the following. For convenience, the system is separated into three parts: a semi-infinite left lead (left region), a scattering region, which includes the molecule and part of the atomic layers in the left and right electrodes, and a semi-infinite right lead (right region). Then, the Hamiltonian matrix $\mathcal{H}$ is given as

$$\mathcal{H} = \begin{pmatrix} H_{\mathrm{L}} & H_{\mathrm{LS}} & 0 \\ H_{\mathrm{SL}} & H_{\mathrm{S}} & H_{\mathrm{SR}} \\ 0 & H_{\mathrm{RS}} & H_{\mathrm{R}} \end{pmatrix}. \tag{1}$$

This Hamiltonian H_{S} of the scattering region is calculated self-consistently within the NEGF/DFT calculation. The overlap matrix $\mathcal{S}$ is written in the same form as equation (1). The Green's function $\mathcal{G}(z)$ is defined by $\mathcal{G}(z) = (z\mathcal{S} - \mathcal{H})^{-1}$, where z is an arbitrary complex number. Then, the retarded Green's function for the scattering region, $G^{\mathrm{r}}_{\mathrm{S}}(\varepsilon)$, is calculated as

$$G^{\mathrm{r}}_{\mathrm{S}}(\varepsilon) = [\varepsilon^{+}S_{\mathrm{S}} - H_{\mathrm{S}} - \Sigma^{\mathrm{r}}_{\mathrm{L}}(\varepsilon) - \Sigma^{\mathrm{r}}_{\mathrm{R}}(\varepsilon)]^{-1}, \tag{2}$$

$$\Sigma^{\mathrm{r}}_{\mathrm{L}}(\varepsilon) = (\varepsilon^{+}S_{\mathrm{SL}} - H_{\mathrm{SL}})G^{\mathrm{r}}_{\mathrm{L}}(\varepsilon)(\varepsilon^{+}S_{\mathrm{LS}} - H_{\mathrm{LS}}), \tag{3}$$

[5] The transport properties are calculated using the ASCOT code, which was developed within the RSS21 project supported by MEXT of the Japanese government. For the details of this code, see [14].

Table 1. Cutoff radius r_{c} of the pseudo-atomic orbitals and number of the primitive orbitals for s, p and d orbitals (n_{s}, n_{p} and n_{d}) used in the calculations.

	r_{c} (au)	n_{s}	n_{p}	n_{d}
Cu	6.0	2	1	1
Ag	6.0	2	1	1
Au	6.0	2	1	1
S	5.5	2	2	2
C	4.0	2	2	—
H	4.0	2	2	—

Table 2. Distance d between the end-group atom S and Y surface in the junction system and the transmission $T(\varepsilon_{\mathrm{F}})$ at the Fermi energy ε_{F} of the electrode.

	d (Å)	$T(\varepsilon_{\mathrm{F}})$
Cu/BPD/Cu	1.591	0.0179
Ag/BPD/Ag	1.760	0.0170
Au/BPD/Au	1.631	0.0525

$$\Sigma^{\mathrm{r}}_{\mathrm{R}}(\varepsilon) = (\varepsilon^{+}S_{\mathrm{SR}} - H_{\mathrm{SR}})G^{\mathrm{r}}_{\mathrm{R}}(\varepsilon)(\varepsilon^{+}S_{\mathrm{RS}} - H_{\mathrm{RS}}), \tag{4}$$

where $G^{\mathrm{r}}_{\mathrm{L/R}}(\varepsilon) = (\varepsilon^{+}S_{\mathrm{L/R}} - H_{\mathrm{L/R}})^{-1}$ is the surface Green's function for the left/right region. The transmission spectrum $T(\varepsilon)$ is then evaluated as

$$T(\varepsilon) = 4\,\mathrm{Tr}\left[\mathrm{Im}\{\Sigma^{\mathrm{r}}_{\mathrm{L}}(\varepsilon)\}G^{\mathrm{r}}_{\mathrm{S}}(\varepsilon)\,\mathrm{Im}\{\Sigma^{\mathrm{r}}_{\mathrm{R}}(\varepsilon)\}G^{\mathrm{a}}_{\mathrm{S}}(\varepsilon)\right], \tag{5}$$

where $G^{\mathrm{a}}_{\mathrm{S}}(\varepsilon)$ and $\Sigma^{\mathrm{r}}_{\mathrm{L/R}}(\varepsilon)$ are the advanced Green's function for the scattering region and the retarded self-energy of the left/right regions, respectively.

In the NEGF/DFT method, the electronic states of the electrodes are taken to be those of bulk fcc Cu, Ag and Au. For a basis set, we employ the pseudo-atomic orbitals, whose cutoff radius r_{c} and number of primitive orbitals are summarized in table 1 [16][6]. We use the PW91 functional parameterized by Perdew and Wang for the exchange–correlation term $V_{\mathrm{xc}}(\mathbf{r})$ [17] and the Troullier–Martins type of atomic pseudopotentials (see footnote 6) [18]. The energy cutoff for the real space mesh is 100 Ryd.

The molecular structure is optimized using Gaussian 03 (PW91PL/LANL2DZ) [19]. The optimization was carried out for an isolated molecule whose S atoms were terminated with H atoms. Then those H atoms were removed and the molecule was sandwiched between metal electrodes. In all the junction systems treated here, the molecule sits upright on the Y(111) surface with the (3 × 3) periodicity and the S atom of each end is located at a hollow site. The distances d between the S atom and the Y surface are set to be those shown in table 2[7].

[6] The pseudo-atomic orbitals are calculated using the CIAO code, which was developed within the RSS21 project.

[7] The distance between the S atom and the Y surface was optimized using the periodic superlattice system consisting of five layers of Y with the (3 × 3) periodicity and a BPD molecule. In this calculation, we used the PHASE code, which is a program package for first-principles total energy calculations based on the density functional theory with a plane wave basis set, developed within the RSS21 project.

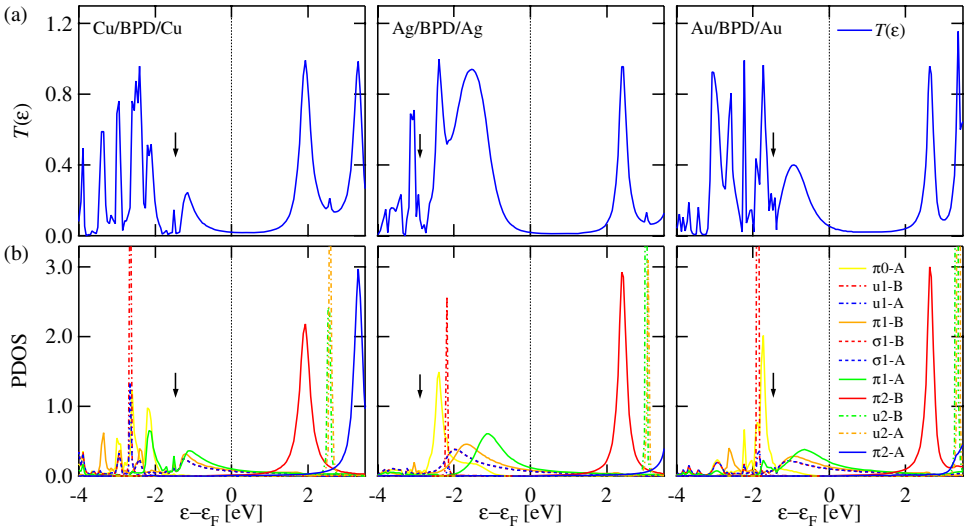

Figure 2. (a) Transmission spectrum $T(\varepsilon)$ for the junction system of the BPD molecule. (b) PDOS with respect to BPD-MOs. The labels, such as π_2-B (A), indicate the name of a constituent fragment MO shown in figure 1(b), and the bonding (B) or anti-bonding (A) state. The d states of the electrode exist below the energy indicated by the arrows.

3. Results and discussion

First, we study the molecular orbital (MO) levels of an isolated BPD molecule. Since the MOs of a BPD molecule are composed of MOs of two equivalent fragments consisting of one phenyl ring and one S atom, we first calculated the MOs of a fragment. Those fragment MOs (f-MOs) are generally classified into σ-type and π-type due to their symmetries. Here, we classify them further for convenience [14]. The σ-type orbital which has great weight on the ring-connecting C atom is named c-type. π-type orbitals that localize in the phenyl ring, especially in the four non-connecting C atoms, are named u-type. It is noted that both c-type and u-type orbitals have much smaller weight on the S atom than the other f-MOs. Eventually, all the f-MOs are classified into the four types. Orbitals of the same type are distinguished by the numbering, as shown in figure 1(b). The MO levels of a BPD molecule are shown in the left part of figure 1(b). The labels, such as π_2-B (π_2-A), indicate the orbital name of a fragment and the bonding (B) or anti-bonding (A) state. It is noted that the mixing of different orbital types, such as σ and π, is quite small. The BPD-MOs consisting of c-type orbitals are shifted out of the energy range shown in figure 1(b), because a c-type orbital has great weight on the ring-connecting C atom and the coupling energy is very large. As a result, there appear just ten BPD-MOs in this energy range. The energy splittings Δ of these orbitals show quite different dependence on the MO symmetry, as shown in the figure. The MOs consisting of π-type orbitals have a large splitting, while the others do not. The small splittings of the latter orbitals reflect the weak interaction between the f-MOs due to the small weight on the ring-connecting C atom. The π_1-type and π_2-type orbitals also exhibit quite different energy splittings.

Next, the electrode metal Y dependence of the transport properties of a BPD molecular junction system is investigated. Figure 2(a) shows the transmission spectrum for Y = Cu, Ag and Au. For all Ys, the transmission spectrum has one broad peak around $\varepsilon - \varepsilon_F \sim -1$ eV and one narrow peak around $\varepsilon - \varepsilon_F \sim 2$ eV. There are many sharp peaks below the energy indicated by the arrows, because the d states of the metal electrodes are located in this energy region. Figure 2(b) shows the projected density of states (PDOS) with respect to the BPD-MOs shown in figure 1(b). The dotted lines indicate the contributions of σ-type MOs. The dotted–dashed lines are for u-type MOs and the solid lines are for π-type MOs. For all Ys, the PDOS with respect to the π_2-B-type MO have a peak around $\varepsilon - \varepsilon_F \sim 2$ eV. For Y = Ag and Au, the PDOS with respect to the π_1-type and σ_1-type MOs have a peak around $\varepsilon - \varepsilon_F \sim -1$ eV. For Y = Cu, the PDOS with respect to the π_1-type and σ_1-type MOs have a peak at $\varepsilon - \varepsilon_F \sim -1$ eV and a few peaks below -2 eV. From the comparison between the PDOSs and the transmission spectrum, it is found that the transmission around $\varepsilon - \varepsilon_F \sim 2$ eV arises from π_2-B-type MO. Besides this, we find that the transmission around $\varepsilon - \varepsilon_F \sim -1$ eV mainly arises from the π_1-type MO. For Y = Ag and Au, the π_0-type MO partially contributes to the transmission around $\varepsilon - \varepsilon_F \sim -1.5$ eV. The σ_1-type MO does not contribute to the transmission, since its level splitting is nearly zero, as shown in figure 1(b).

Here, we investigate a relation between PDOS peak energies, transmission and MO states. The PDOS peak width for the u-type MO is very narrow, indicating that the interaction between the u-type MO and the electrode is nearly zero. This reflects the fact that the weight on the S atom of the MO is quite small [14]. Therefore, from the peak energy of the PDOS with respect to the u-type MOs, we can estimate a general energy level of the BPD-MOs with respect to the Fermi energy for each Y, that is mainly determined by the vacuum level and the charge transfer between a molecule and the electrodes. From this, we find that the MOs for Y = Cu are located in the lower energy side and the MOs for Y = Au are located in the higher energy side. As a result, for Y = Cu, the π_1-type and σ_1-type MOs strongly hybridize with the d states of the electrodes

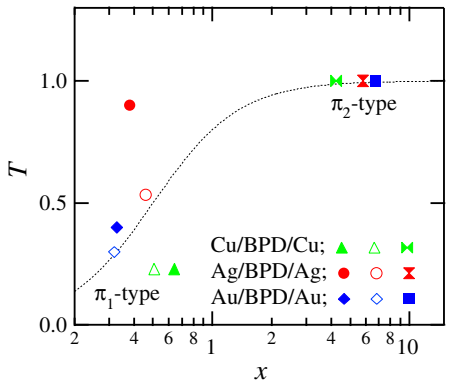

Figure 3. Transmission value T at the energy of the peak center of the PDOS against $x = \Delta/W$. The closed (opened) markers show bonding (anti-bonding) orbitals. The dotted line shows $T(x) = 4x^2/(4x^2+1)$.

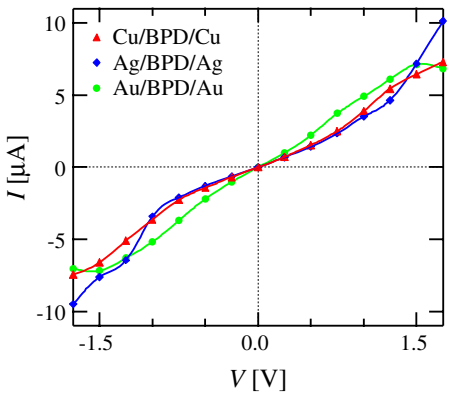

Figure 4. I–V curve for a BPD molecular junction system with Y = Cu, Ag and Au.

and then several peaks appear in the PDOSs, considering the fact that the d states of the metal electrodes are located at $\varepsilon - \varepsilon_F < -2.9$ eV for Ag and $\varepsilon - \varepsilon_F < -1.5$ eV for Cu and Au. It is found that the system with Y = Au has the largest transmission at the Fermi energy, as shown in table 2. This is a result of the difference in a PDOS peak energy for the π_1-type MOs, which mainly contributes to the transmission at the Fermi energy. Meanwhile, the transmission at the Fermi energy for Y = Cu is almost equal to that for Y = Ag, although the PDOS peak energies for the π_1-type MOs are different. This is because the PDOS with respect to the π_1-type MO for Y = Cu spreads over a wider energy range.

Next, we discuss transmission peak values. This value depends on the coupling between MOs on the phenyl rings and the interactions between the molecule and the electrode, which are defined for each MO [15]. The coupling between MOs on the phenyl rings is estimated from the level splitting Δ shown in figure 1(b). The molecule–electrode interaction is estimated from a PDOS peak width (W) shown in figure 2(b). Namely, a broader PDOS peak means a stronger interaction between a MO and an electrode [20]. From this, we find that the interaction between the π_1-type MO and the electrode for Y = Au is stronger than that for Y = Ag. For the π_1-type MO in the case of Y = Cu, we cannot estimate the interaction from the PDOS peak width, since the π_1-type MOs hybridize with the d state of the Cu and, as a result, the PDOS has a multi-peak structure. However, we expect the interaction for the π_1-type MO to also be stronger than that for Y = Ag, because the PDOS peaks spread over a wide energy range. It is also found that for all Ys, the interaction between the π_2-type MO and the electrode is weaker than that between the π_1-type MO and the electrode. There is a report that for a Au electrode system, a transmission value at the peak center of the PDOS can be expressed well as $T(x) = 4x^2/(4x^2+1)$, where $x = \Delta/W$.[8] According to this equation, a larger W and a smaller Δ give a smaller transmission value. Figure 3 shows x versus the transmission value at the peak center of the PDOS, extracted from figures 1 and 2. Each value agrees well with the ideal value $T(x)$ except for the π_1-type MO in the case of Y = Cu and the π_1-B-type MO in the case of Y = Ag. From this relation, we can understand how the transmission peak values are determined, as follows: the transmission value at $\varepsilon - \varepsilon_F \sim 2$ eV is 1, since the peak width of the PDOS with respect to the π_2-B-type MO is narrow and then x is large. The transmission peak value around $\varepsilon - \varepsilon_F < -1.5$ eV for Y = Ag is larger than that for Y = Au, since the peak width of the PDOS with respect to the π_1-type MO for Y = Ag is narrower. As described above, the π_1-type MO in the case of Y = Cu and the π_1-B-type MO in the case of Y = Ag does not agree with $T(x)$. This discrepancy can be understood as follows: (i) for the π_1-type MO in the case of Y = Cu, the PDOS has a multi-peak structure, since the MO strongly hybridizes with the d state of Cu. This result in an underestimate of the peak width W and an overestimate of x. Comparing the transmission peak value with $T(x)$ with a smaller x, we would obtain a better agreement. (ii) For π_1-B-type MO in the case of Y = Ag, the transmission at the peak center of the PDOS with respect to π_1-B-type MO partially arises from the π_0-type MO, as shown in figure 2. In such a case, it is difficult to extract fairly the contribution of one MO to the transmission. In this way, it is found that the relation between a transmission value and x, suggested for a Au electrode system, is applicable for different metal electrodes.

Finally, we investigate the transport properties under finite bias voltage via self-consistent calculation. In figure 4, we show the electrode metal Y dependence of the I–V curve. For Y = Au, we obtain a linear behavior in a bias range of 0 V $< V <$ 1.5 V and the current value saturates around $V = 1.5$ V. For Y = Cu, we observe a linear behavior in a bias range of 0 V $< V <$ 1.5 V and a smaller current value than that for Y = Au is obtained. This arises from the smaller transmission around the Fermi energy. For Y = Ag, we also obtain a smaller current value than that for Y = Au in a bias range of 0 V $< V <$ 1.5 V for the same reason as for the case of Y = Cu. In a bias range of $V > 1.5$ V, we obtain larger current values for Y = Ag than for Y = Au, since for Y = Ag higher transmission is obtained around $\varepsilon - \varepsilon_F \sim -1.5$ eV, as shown in figure 2.

[8] $T(x)$ is obtained from an analysis for a simple one-dimensional chain model [13], which is an effective model for a BPD molecular junction system. The details are reported in [15].

The change in the transmission spectrum on changing the electrode metal has not been reported from any experiments. As discussed above, this change arises from the difference in the PDOS peak energy and that in the strength of the molecule–electrode coupling. Here, it is noted that recent developments in experiments can give high resolution differential conductance with high reproducibility [21]. Such a differential conductance can be treated as an approximate transmission spectrum around the Fermi energy. We expect that from it, the electrode metal dependence of the transmission spectrum reported in the present paper would be confirmed.

4. Conclusions

In summary, we have studied the transport properties of a BPD molecule sandwiched between metal electrodes (Y = Cu, Ag and Au) using an NEGF/DFT method and the electrode metal effects have been investigated. By changing the electrode metal, the PDOS peak energy and the coupling between the molecule and the electrodes are changed. For Y = Ag, we observe a larger transmission peak value than that for Y = Au, since the interaction between the molecule and the Ag electrodes is weaker than that for Au electrodes. The transmission at the Fermi energy ε_F is smaller than that for Y = Au. This is because, in the system with Y = Ag, MO levels below ε_F are located far from ε_F and the transmission peak is narrower. At high bias voltage, the current value for Y = Ag is larger than that for Y = Au, because the system with Y = Ag has a higher transmission peak around $\varepsilon - \varepsilon_F \sim -1.5$ eV. For Y = Cu, we obtain almost the same transmission value at ε_F as for the system with Y = Ag, although the PDOS peak energies for the π_1-type MO are different. This is because the interaction between the molecule and the Cu electrodes is stronger than that for Ag electrodes. Besides this, it is found that the expression $T(x) = 4x^2/(4x^2 + 1)$, where $x = \Delta/W$, for evaluating a transmission peak value is general for all Ys considered here.

Acknowledgments

This study was partially supported by a Grant-in-Aid for Scientific Research (No. 17064017) and the RISS project of MEXT of the Japanese Government. The present calculations were performed by using the Numerical Materials Simulator in NIMS.

References

[1] For a theoretical review: Koentopp M, Chang C, Burke K and Car R 2008 *J. Phys.: Condens. Matter* **20** 083203 and references therein
[2] For an experimental review: McCreery R L 2004 *Chem. Mater.* **16** 4477 and references therein
[3] Xu B and Tao N J 2003 *Science* **301** 1221
Venkataraman L, Klare J E, Nuckolls C, Hybertsen M S and Steigerwald M L 2006 *Nature* **442** 904
[4] Aviram A and Ratner M A 1974 *Chem. Phys. Lett.* **29** 277
Joachim C, Gimzewski J K and Aviram A 2000 *Nature* **408** 541
[5] Babiaczyk W I and Bulka B R 2004 *J. Phys.: Condens. Matter* **16** 4001
Rocha A R, García-Suárez V M, Bailey S W, Lambert C J, Ferrer J and Sanvito S 2005 *Nat. Mater.* **4** 335
Dalgleish H and Kirczenow G 2005 *Phys. Rev.* B **72** 184407
[6] Yaliraki S N, Kemp M and Ratner M A 1999 *J. Am. Chem. Soc.* **121** 3428
[7] Seminario J M, De La Cruz C E and Derosa P A 2001 *J. Am. Chem. Soc.* **123** 5616
[8] Geng W T, Nara J and Ohno T 2004 *Thin Solid Films* **464/465** 379
[9] Lawson J W and Bauschlicher C W 2006 *Phys. Rev.* B **74** 125401
[10] Tomfohr J K and Sankey O F 2002 *Phys. Status Solidi* **233** 59
[11] Samanta M P, Tian W, Datta S, Henderson J I and Kubiak C P 1996 *Phys. Rev.* B **53** 7626
[12] Pauly F, Viljas J K, Cuevas J C and Schön G 2008 *Phys. Rev.* B **77** 155312
[13] Kondo H, Nara J, Kino H and Ohno T 2008 *J. Chem. Phys.* **128** 064701
[14] Kondo H, Nara J, Kino H and Ohno T 2008 *Japan. J. Appl. Phys.* **47** 4792
[15] Kondo H, Nara J and Ohno T 2008 in preparation
[16] Ozaki T 2003 *Phys. Rev.* B **67** 155108
[17] Perdew J P and Wang Y 1992 *Phys. Rev.* B **45** 13244
[18] Troullier N and Martins J L 1991 *Phys. Rev.* B **43** 1993
Kleinman L and Bylander D M 1982 *Phys. Rev. Lett.* **48** 1425
[19] Frisch M J *et al* 2004 (Wallingford, CT: Gaussian)
[20] Kondo H, Kino H, Nara J, Ozaki T and Ohno T 2006 *Phys. Rev.* B **73** 235323
[21] For example Reichert J, Weber H B, Mayor M and von Löhneysen H 2003 *Appl. Phys. Lett.* **82** 4137